THE JOURNAL OF PHYSICAL CHEMISTRY B

Article

pubs.acs.org/JPCB

Crystallite Width Determines Monolayer Hydration across a Wide Spectrum of Celluloses Isolated from Plants

Carlos Driemeier* and Juliano Bragatto†

Laboratório Nacional de Ciência e Tecnologia do Bioetanol − CTBE/CNPEM Caixa Postal 6170, 13083-970, Campinas, São Paulo, Brazil

Supporting Information

ABSTRACT: Relating cellulose structure to its water uptake is a classical problem with many investigations done through measurements of cellulose "crystallinity". However, there is presently a growing consensus that crystallinity measurements are appreciably uncertain, leading to ambiguous interpretations of underlying cellulose organization. In this scenario, this article revisits the relations between cellulose structure and water uptake, moving the emphasis away from degree of crystallinity and directing it toward crystallite width, which is inferred with less ambiguity from the broadening of 200 X-ray diffraction peaks. With this approach, analysis of a wide spectrum of celluloses isolated from plants (preserving cellulose I phase and having variable contents of residual hemicelluloses) reveals a simple linear relation (R^2 = 0.98) between reciprocal crystallite width and monolayer hydration (determined from vapor sorption). The primary role of crystallite width supports that most water-accessible polysaccharides are laterally associated with the crystallites, with a minor fraction in disordered domains along the fibrils. Furthermore, the secondary role left to hemicellulosic contents indicates cellulose being partly decrystallized to complement the disordered amount required to interface the crystallites. Finally, a substantial part of hydration is attributed to polysaccharides in voids left by the imperfect packing of aggregated crystallites.

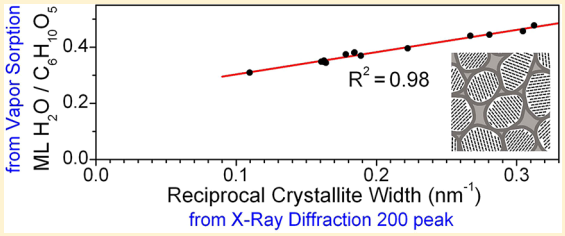

1. INTRODUCTION

Water is ubiquitous, and cellulose is the most abundant biopolymer on Earth. These two components interact in scales that span water hydrogen bonding to cellulose (molecular scale), water filling of cellulose pores (capillarity), and macroscopic cellulose volume gains (swelling). This brief presentation highlights that cellulose−water interactions have major fundamental as well as technological importance. Against this panorama, the present study is focused on the cellulose first hydration layer, the so-called monolayer (ML), which estimates the amount of water in direct molecular contact with the solid matrix. Furthermore, for reasons that will be explained, the scope of the article is limited to processed plant celluloses that retain the native crystal phase (cellulose I), which is stabilized[1,2] in the structure of cellulose I_β.[3]

In plant cell walls, hydration takes place between cellulose microfibrils, spacing them apart from one another. This is the microscopic phenomenon behind the directional (perpendicular to microfibrils) hygroexpansion of woods[4] and movements of plant organs induced by changes in relative humidity (RH).[5] In systems with paralleled and regularly packed microfibrils, center-to-center microfibril distances (3−5 nm) have been estimated by small-angle X-ray or neutron scattering. Increasing microfibril distances due to hydration were observed for spruce wood[6] and celery collenchyma.[7] In these materials, cellulose microfibrils may be primarily spaced by matrix components (hemicelluloses, lignin, pectins), and the observed interfibrillar hydration may be specific to these interfibrillar matrixes. For cellulose isolated from celery collenchyma, however, appreciable microfibril spacing upon hydration was not observed.[7] With a different approach that employed inelastic neutron scattering, a common dynamic signature was observed for disordered, water-accessible regions of several native celluloses.[8]

In other purer forms of cellulose, early attempts to understand water uptake assumed water sorption primarily on the "amorphous" fraction of cellulose. On the basis of this assumption, Hailwood and Horrobin[9] analyzed vapor sorption (VS) isotherms with their polymer hydration model, and used the results to infer the degree of crystallinity of cotton cellulose. Following a similar line of thought, Hermans and Weidinger[10,11] applied their X-ray diffraction (XRD) method for estimation of the cellulose degree of crystallinity and related this property with water gains (in 65% RH) in raw and acid-hydrolyzed ramie cellulose. These early works, however, explored little of cellulose structural variability.

More recently, water sorption in cellulose was investigated across a wider structural spectrum, including microcrystalline and decrystallized (by milling) celluloses isolated from plants as well as celluloses from algae.[12,13] For plant celluloses, areas available for water sorption (~100 m^2/g) were 2 orders of magnitude higher than areas available for nitrogen sorption (~1

Received: October 8, 2012
Revised: December 10, 2012
Published: December 20, 2012

m^2/g, measured in dry samples). This was explained by interfibrillar penetration of water but not of nitrogen. In Strømme et al.,[14] fractal dimensions were included in sorption analysis. In Mihranyan et al.,[12] ML hydration was shown to inversely depend on cellulose crystallinity index, as measured by the peak-high Segal method.[15]

A major limitation of the studies presented in the last two paragraphs is that they rely on measurements of cellulose "crystallinity". These measurements are highly uncertain and elusive, with results strongly dependent on the measurement method.[16] Concerning analysis by XRD, our research group has recently shown[17] the critical corrections for preferential orientation, incoherent scattering, and moisture content, necessary if degree of crystallinity as mass-fraction crystal content is to be obtained. The importance of peak profile functions used in XRD modeling has also been recognized,[17,18] as previously noted by Hindeleh and Johnson.[19] Furthermore, the "amorphous" components associated with cellulose are preferentially aligned to the crystallites[20,21] and do not correspond to the ideal isotropic amorphous lacking long-range atomic order. Hence, the "amorphous" contribution to diffraction patterns should be judged with care. Other common analysis of cellulose crystallinity is done in the C4 spectral region of ^{13}C solid-state nuclear magnetic resonance (NMR). In this technique, part of the "amorphous" signal is due to cellulose chains at crystallite surfaces,[22] which, from an XRD perspective, likely take part of the crystals. Indeed, by exploiting NMR relaxation times, the ratio between NMR signals of crystal cores and surfaces was shown to be well correlated with the *width* of crystallites measured by XRD.[23]

Mean crystallite width can be inferred from broadening analysis of equatorial X-ray diffraction peaks. Crystallite width depends on source and processing of plant cellulose. Width is ≈3 nm in raw lignocellulose, increases upon pulping and acid hydrolysis, and is even wider (up to ≈9 nm) in raw and treated cotton cellulose.[18,24,25] In plant cell walls, cellulose is thought to be synthesized by individualized rosettes, forming individualized microfibrils.[26] Crystallites ≈3 nm wide are broadly consistent with 24−36 cellulose chains synthesized within a rosette.[6] Nevertheless, the wider crystallites found in cotton, bast fibers, tension wood, and celluloses isolated from lignocellulose are not consistent with this picture. Concerning crystallite widening in wood pulping, Ioelovitch[24] argued that cellulose microfibrils lose their individuality. Reduction of crystallite specific surface area is likely a thermodynamic driver for crystallite widening, but mechanisms of widening remain unclear. Lower amounts of noncellulosic components (in the raw cell wall or after processing) is usually a condition found associated to wider cellulose crystallites.[18,24,27]

The present article compares monolayer hydration determined by vapor sorption to degree of crystallinity and crystallite width determined by X-ray diffraction. Uncertainties in degree of crystallinity are explicitly recognized. Hence, differing from previous studies, relations between cellulose structure and water uptake are focused on crystallite width, which is estimated with less ambiguity. With this approach, analysis of a wide spectrum of celluloses isolated from plants presents a simple linear relation (R^2 = 0.98) between ML hydration and reciprocal crystallite width. Aided by estimates of degree of crystallinity, implications of this finding are discussed.

2. MATERIALS AND METHODS

2.1. Cellulose Samples. Celluloses were acquired from commercial suppliers, kindly provided by collaborators, or processed in our laboratory. From Sigma-Aldrich (catalog code in parentheses), we acquired Fluka cellulose (22183), Sigmacell type 20 (S3504), Sigmacell type 50 (S5504), Avicel PH-101 (11365), Sigmacell type 101 (S6790), and α-cellulose (C8002). In addition, we acquired Celufloc 200 (from Celuflok), Whatman #1 filter paper, and two bleached Eucalyptus kraft pulps (from Brazilian mills). A bleached Eucalyptus pulp produced in subcritical ethanol−water−CO_2 mixture[28] was kindly provided by Dra. M. T. B. Pimenta. Peracetic pulps from sugar cane bagasse were produced in a 1:1 mixture of 8.74 M glacial acetic acid and 21.6 M hydrogen peroxide at 60 °C for 15, 24, or 48 h. These 14 materials were named Fluka, S20, S50, Avicel, S101, Alpha, Floc, FP, Ekp1, Ekp2, Esc, Bpa15, Bpa24, and Bpa48, respectively. All samples were handled in laboratory atmosphere, becoming air-dried before XRD and VS analysis. The samples form a heterogeneous set that is appropriate to explore relations valid across a wide spectrum of materials.

2.2. Compositional Analysis. Material composition was measured by a standard protocol[29] in which the solid samples were submitted to two-step analytical acid hydrolysis. Sugar concentrations in the hydrolysates (cellobiose, glucose, xylose, arabinose, galactose, and mannose) were measured by liquid chromatography and converted to dry-basis (g/g) cellulose and hemicellulose contents in the solids. The standard protocol[29] was modified to replace the corrective sugar recovery standards by measured concentrations of glucuronic, formic, and acetic acids, furfural and hydroxymethylfurfural.

2.3. X-ray Diffraction. XRD was performed as in previous studies.[17,18] Air-dried samples were conditioned in capillary tubes and analyzed in fiber geometry using a Rigaku ultraX-18HF rotating anode generator with Cu Kα radiation (λ = 1.5418 Å), VariMax HR monochromating optics, and mar345 image plate (positioned 120 mm behind samples). The two-dimensional diffraction patterns were analyzed by the Rietveld method[30] using the MAUD program.[31] The degree of crystallinity, defined as crystal mass per sample dry mass, was estimated following previous developments,[17] which included corrections for incoherent scattering, sample moisture content, crystal texture, blank intensity, and X-ray absorption.

In the employed Rietveld procedure, line-broadening analysis accounted for instrumental as well as specimen contributions. Instrumental line broadening was calibrated with α-alumina. Specimen line broadening for the major equatorial peaks ($1\underline{1}0$, 110, and 200) was modeled by Lorentzian profiles, following the Delft line-broadening model.[32] Mean crystallite width in the [200] direction (L_{200}) was derived from the Rietveld analysis, which had been verified to employ the Scherrer equation

$$L_{200} = \frac{K\lambda}{B_{200}\cos\theta} \quad (1)$$

where B_{200} is the full width at half-maximum of the specimen contribution to the 200 peak width and the shape factor is K = 1.1.

2.4. Vapor Sorption. VS analysis was performed in a Q5000 SA (from TA Instruments) instrument, as detailed elsewhere.[33] Samples of about 5 mg held in a metalized quartz pan were initially equilibrated at 50 °C, 0.95 RH. Then, the RH was stepped down for water desorption and, after complete sample drying, RH was stepped up for water sorption. Sample

dx.doi.org/10.1021/jp309948h | J. Phys. Chem. B 2013, 117, 415−421

mass was monitored continuously. Each RH step took 60 min, except at RH = 0, which was kept for 180 min to improve the definition of sample dry mass. Desorption and sorption isotherms were built from water contents (per unit of dry mass) at the end of each RH step.

Desorption and sorption isotherms were analyzed by the Brunauer–Emmett–Teller (BET)[34] and the Hailwood–Horrobin (HH)[9] models. The BET model analyzes isotherms through two coefficients: ML mass and ML interaction constant. To generate satisfactory fits, application of the BET model was restricted to RH $\leq$ 0.4. The HH model analyzes isotherms through three coefficients: ML mass, ML interaction constant, and an additional interaction constant for the so-called dissolved water (beyond ML water). Hence, the HH model, with its additional coefficient, provided a more complete description of hydration. The HH model was applied to RH $\leq$ 0.8. Application of the HH model to sorption analysis of celluloses was further detailed elsewhere.[33] For a review of hydration models, see the book by Skaar.[4]

3. RESULTS

Figure 1 compares diffractograms and water sorption isotherms from selected samples. The diffractograms are presented in the region of 1$\underline{1}$0, 110, and 200 equatorial reflections, from where crystallite widths can be derived by application of the Scherrer equation. The 200 peak is the best to estimate crystallite width because this peak is more intense and peak overlapping is not critical as it is for 1$\underline{1}$0 and 110. Moreover, diffractograms of Figure 1 evidence that width changes in 200 peaks are concomitant to width changes in 1$\underline{1}$0 and 110 peaks (the Supporting Information compares inferred crystallite widths). Crystallite width L_{200} is, therefore, representative of crystallite lateral dimensions. Since 1$\underline{1}$0 and 110 widths are harder to quantify because of overlapping, L_{200} is the only width employed henceforth. Figure 1 also evidences that less water is sorbed in samples presenting sharper 200 diffraction peaks (due to wider crystallites). However, differences in water contents among samples are modest compared to differences in 200 peak width.

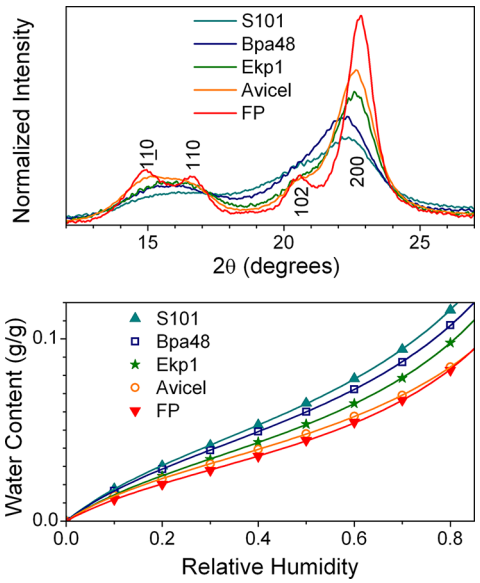

Figure 1. X-ray diffractograms and vapor sorption isotherms for selected samples. To ease visual comparison, presented diffractograms (top) are those with closest similarity to isotropic reconstructions of experimentally anisotropic (due to cellulose preferential orientation) area-detector diffraction patterns; in addition, presented diffractograms are subtracted out of Rietveld-resolved backgrounds and are normalized to equal peak areas. Sorption isotherms (bottom) show experimental data (symbols) and fits with the Hailwood–Horrobin model (lines).

The investigated sample set nearly covers the full range of crystallite width observed in cellulose isolated from plants, with measured L_{200} between 3.2 and 9.1 nm (see Table 1). In one extreme (L_{200} < 4.0 nm), crystallites from S101 and Bpa15, Bpa24, and Bpa48 are only slightly wider than in raw lignocellulose. In the other extreme (L_{200} > 6.0 nm), FP, Avicel, and Fluka are made from cotton linters (as informed by manufacturers) and, because of structural and compositional similarities (see Table 1), S20 and S50 are presumed to be from cotton linters as well. Regarding composition, for all samples, the major component is cellulose (0.68–0.99 g/g), complemented by hemicelluloses (0.02–0.29 g/g), with xylan being the major hemicellulose of all samples. Contents of total lignin, insoluble (acid insoluble residue subtracted out of ash content) plus soluble (measured by ultraviolet absorbance), are negligible (<0.01 g/g). Part of the data from Table 1 was published previously in different contexts.[33,35] (Note: a different method of compositional analysis was employed in ref 35.)

Figure 2 compares three estimates of water ML, shown as a function of reciprocal crystallite width (later the reason for this horizontal axis will become clear). The first estimate is water ML determined from sorption isotherms with the HH model, and the second, with the BET model. It is noteworthy that the BET model has been criticized[13,36] because its assumption of multilayer sorption is unrealistic at solid–solid interfaces. The third estimate is direct reading of sorption isotherms at 0.3 RH. This RH was chosen because, at low RH, water content is dominated by ML, while, at higher RH, capillarity (pore water) is increasingly important.[13,33] Precisions (1σ) in these measurements of water content are better than 0.0006 g/g, as inferred from replicate analyses.

The three measurements of water content (Figure 2) present the same basic trend: a linear relation with positive intercept and slope and high coefficient of determination ($R^2 \geq 0.95$). Indeed, analysis of desorption (instead of sorption) isotherms shows a similar linear trend, but coefficients of determination are lower (R^2 = 0.91 for the HH model, based on the data of Table 1). This is attributed to the influence (in desorption analysis) of water pockets inherited from water-swollen states.[33] Considering the general agreement of the different water ML estimates, the discussion follows based on the observed ML × $1/L_{200}$ linear trend with positive intercept and slope. Moreover, henceforth we discuss only water ML determined by the HH model (more complete and appropriate model) applied to *sorption* isotherms (less influenced by water in pores). This estimate of water ML has the best linearity with $1/L_{200}$ (R^2 = 0.98, see Figure 2).

One important consideration is that crystallite width derived by XRD accounted for instrumental broadening (see Materials and Methods), but polymers have an additional contribution to diffraction peak broadening due to defects of the second kind (paracrystallinity).[37] Paracrystallinity is here understood as fluctuations of interplanar spacing within a crystallite, not the disordered regions at a cellulose crystallite surface, which are sometimes termed "paracrystalline".[38] Following the ideal

dx.doi.org/10.1021/jp309948h | J. Phys. Chem. B 2013, 117, 415–421

Table 1. Complete Data Set Discussed in the Article, with Parameters from X-ray Diffraction (Crystallite Width L_{200} and Degree of Crystallinity x_{cr}), Vapor Sorption (Hailwood−Horrobin Monolayer (HH ML), Brunauer−Emmett−Teller Monolayer (BET ML), Water Content at 0.3 Relative Humidity (RH), and Hailwood−Horrobin Monolayer from Desorption (HH ML_d)), and Composition (Cellulose and Hemicellulose Contents)

	X-ray diffraction		vapor sorption				composition	
sample	L_{200} (nm)	x_{cr} (g/g)	HH ML (g/g)	BET ML (g/g)	@0.3 RH (g/g)	HH ML_d (g/g)	cellulose (g/g)	hemi (g/g)
S101	3.20	0.49	0.0530	0.0397	0.0415	0.0650	0.764	0.194
Bpa15	3.28	0.61	0.0507	0.0381	0.0395	0.0617	0.679	0.285
Bpa24	3.56	0.68	0.0494	0.0367	0.0378	0.0583	0.761	0.251
Bpa48	3.75	0.65	0.0489	0.0369	0.0389	0.0562	0.803	0.196
Alpha	4.50	0.56	0.0440	0.0327	0.0346	0.0509	0.810	0.199
Floc	5.42	0.72	0.0423	0.0316	0.0339	0.0481	0.857	0.146
Ekp1	5.43	0.76	0.0422	0.0326	0.0339	0.0489	0.827	0.168
Ekp2	5.61	0.84	0.0416	0.0324	0.0344	0.0476	0.830	0.148
Esc	5.29	0.69	0.0411	0.0315	0.0336	0.0463	0.941	0.054
S20	6.15	0.78	0.0391	0.0292	0.0315	0.0429	0.955	0.025
S50	6.22	0.85	0.0387	0.0289	0.0312	0.0424	0.941	0.036
Fluka	6.15	0.81	0.0386	0.0288	0.0314	0.0418	0.972	0.023
Avicel	6.10	0.80	0.0383	0.0290	0.0314	0.0430	0.985	0.024
FP	9.12	0.76	0.0344	0.0268	0.0279	0.0441	0.940	0.025

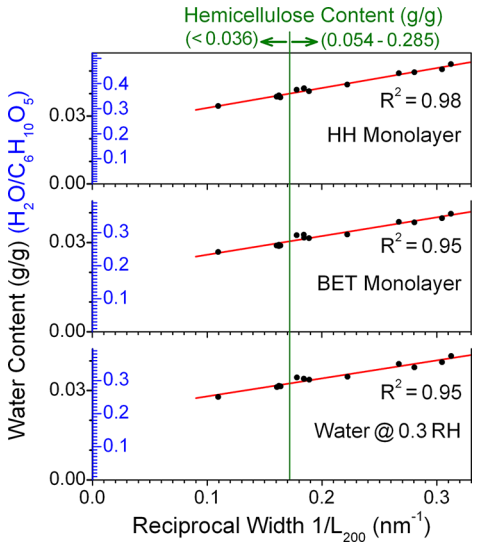

Figure 2. Water content versus reciprocal crystallite width $1/L_{200}$. Water contents are presented in units of water mass per sample dry mass (g/g) as well in units of water molecules per anhydroglucose unit ($H_2O/C_6H_{10}O_5$), as converted by formula masses. Water contents are monolayers derived from sorption isotherms by employing the Hailwood−Horrobin (HH) model (top) or the Brunauer−Emmett−Teller (BET) model (middle), or simply water contents measured in 0.3 relative humidity (RH) (bottom). The vertical green line marks a step change in hemicellulose contents. Red lines are linear fits whose coefficients of determination (R^2) are indicated.

paracrystal model,[39] paracrystalline broadening is proportional to g^2/d, where g is the paracrystalline distortion parameter and d is the interplanar spacing. However, g also follows a scaling law (named the α^* relation),[39] $g^2 = \alpha^{*2}d/L$, where α^* is a constant and L is the mean crystallite size. Therefore, paracrystalline broadening is also proportional to $1/L$, as size broadening is, and, for a given *hkl* reflection, paracrystalline broadening makes an approximate constant fraction of peak width. That is, the primary effect of paracrystallinity is to increase K in eq 1, and correcting L_{200} for paracrystallinity would change the ML × $1/L_{200}$ slope but would preserve its intercept (see Figure 2).

An implication of the remarkable ML × $1/L_{200}$ linear trend is the secondary role left to hemicellulose content as a variable explanatory of water uptake. This may contradict expectations, because hemicelluloses are presumably "amorphous" and hydrated. The secondary role of composition is further evidenced in two ways. First, there is a minor deviation from the ML × $1/L_{200}$ linear trend upon crossing the vertical green line of Figure 2, which marks a step change in hemicellulose content. (The line divides celluloses from cotton and from lignocellulose.) Second, a linear fit to water ML × hemicellulose content (Figure 3) brings a comparatively modest

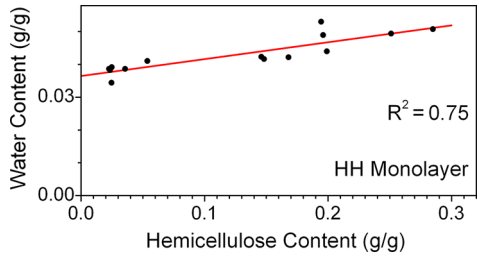

Figure 3. Monolayer water versus hemicellulose content. Monolayer water was derived by analyzing sorption isotherms with the Hailwood−Horrobin (HH) model. The red line is a linear fit whose coefficient of determination (R^2) is indicated.

coefficient of determination (R^2 = 0.75). It is worth recalling that a low amount of noncellulosic components is a condition typically found associated to wider cellulose crystallites.[18,24,27] Hence, the existing correlation between water ML and hemicellulose content (Figure 3) is likely a consequence of this association between composition and crystallite width. Finally, there is substantial variation in water ML that appears uncorrelated to hemicellulose contents between 0.15 and 0.20 g/g (see Figure 3). Quantitative discrimination between the primary role of crystallite width and the secondary role of hemicellulose content may be achievable assuming a multivariate model for hydration, which is beyond the scope of the present study.

Measurements of the degree of crystallinity can provide further insight about the pattern of water sorption in celluloses.

dx.doi.org/10.1021/jp309948h | J. Phys. Chem. B 2013, 117, 415−421

Figure 4 presents degree of crystallinity versus $1/L_{200}$. The *y*-axis scale is inverted so amorphous (noncrystalline) contents in

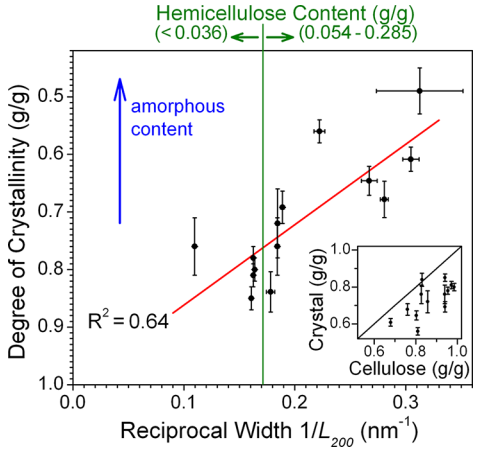

Figure 4. Degree of crystallinity versus reciprocal crystallite width $1/L_{200}$. The *y*-axis scale is inverted, so amorphous content increases to the top. The vertical green line marks a step change in hemicellulose content. The red line is a linear fit whose coefficient of determination (R^2) is indicated. Error bars are 1σ precisions, as inferred from replicated analysis. The inset presents the degree of crystallinity versus cellulose content (*y*-axis scale not inverted), with data points at or below the $y = x$ line.

Figure 4 can be visually compared to water contents in Figure 2. Before discussing measured degrees of crystallinity, one must recognize that their uncertainties are much larger than for water ML and L_{200}. In Figure 4, error bars for $1/L_{200}$ (horizontal) and degree of crystallinity (vertical) are 1σ precisions inferred from repeated measurements with the constant analytical procedure. The error bars do not account for uncertainty in peak profile functions, recognized[17−19] to be significant for cellulose crystallinity measurements. The horizontal error bars typically increase with $1/L_{200}$ because broader XRD peaks are poorly defined. Furthermore, $1/L_{200}$ precision is poorer when inferred from more isotropic two-dimensional XRD patterns (less crystallite texture). This is the case of the S101 sample that presents the larger $1/L_{200}$ error bars (topmost data point of Figure 4).

Three features related to degree of crystallinity are worth noting. *First,* degrees of crystallinity are equal or lower than cellulose contents (inset of Figure 4), indicating the presence of amorphous cellulose in addition to noncellulosic amorphous. Therefore, amorphous (and presumably hydrated) polysaccharides include amorphous cellulose, which explains the secondary role that hemicellulose content *per se* has on water uptake. *Second,* there is no substantial change in degree of crystallinity upon crossing the vertical green line of Figure 4, which marks a step change in hemicellulose content. This suggests that amorphous cellulose is complementing amorphous hemicellulose, possibly to yield a required amount of total amorphous. *Third,* data points in Figure 4 present a positive slope consonant with the positive slope observed in Figure 2. This slope indicates amorphous polysaccharides associated with crystallite surfaces. Dispersion of data points around the fitted line and the associated modest coefficient of determination (R^2 = 0.64) may primarily result from uncertainties in degree of crystallinity measurements.

4. DISCUSSION

4.1. Implications of the Primary Role of Crystallite Width. Figure 2 evidences that ML hydration is primarily determined by crystallite width, which is a lateral dimension of the crystallites. The role of crystallite width on cellulose hydration was earlier proposed by Kocherbitov et al.;[13] they however did not include in the model the positive intercepts presented in Figure 2. The primary role of crystallite width is a notable evidence that hydration is majorly associated to the sides of the crystallites, with minor fraction in disordered domains along the fibrils. In numerical terms, R^2 = 0.98 indicates that approximately 98% of the variance in ML hydration is explained by crystallite width alone, with 2% left to other uncorrelated sources of variance (including finite experimental precision). Hence, hydration in sites unassociated to crystallite sides would be limited to about a few percent of the total hydration. Our result is in agreement with the quantitative investigation[40] of disordered regions along ramie microfibrils, which evidenced that disordered domains are limited to a few percent of microfibril lengths. Our finding extends the evidence to a much broader spectrum of celluloses.

Associated with the issue of disordered domains along fibrils, there is controversy about the typical length of cellulose crystallites. XRD line broadening analysis reports crystallites 20−40 nm long,[25] but these lengths may be critically underestimated because other contributions to broadening (microstrain, paracrystallinity, crystallite twist) are of magnitudes comparable to size broadening. Alternatively, judging from the lengths of isolated nanoparticles[41−43] and from the periodicity of disordered regions along ramie microfibrils,[40] crystallite lengths are estimated to be of the order of hundred nanometers. Our results are better consistent with such longer crystallites.

For ML hydration, hemicellulose content has a role secondary to crystallite width, which may be surprising because hemicelluloses are thought to be "amorphous" and hydrated. Our results do not contradict that hemicelluloses are amorphous and hydrated. They rather reveal that cellulose itself may be as amorphous and hydrated as hemicelluloses are. We understand that "amorphousness" is a structural requirement associated with interfaces between crystallites. Wherever required, cellulose is partly decrystallized to complement hemicelluloses, forming the total amount of disordered polysaccharide required to interface neighbor crystallites aggregated into bundles.

4.2. Specificities of Celluloses Isolated from Plants. The scope of the present work is limited to celluloses isolated from plants, having cellulose I crystal phase and negligible lignin. In addition to the high aspect ratio (length/width) of the crystallites, there are other key specificities to explain the observed relation between crystallite width and ML hydration. (i) Since celluloses were processed, compounds in highly reactive configurations were likely removed, leaving the less reactive configurations, which tend to be those condensed in the solid state. (ii) Since lignin content is negligible, materials are majorly made of structural polysaccharides (cellulose and hemicelluloses). Their molecular features critical for water sorption (e.g., per-mass sites for hydrogen bonding) are quite similar, with the dominant difference relating to their packing (or not) into crystallites. (iii) Crystallite aggregation into bundles (also termed aggregates or macrofibrils)[44−47] seems to be intrinsic to plant cellulose (but not necessarily to other

dx.doi.org/10.1021/jp309948h | J. Phys. Chem. B 2013, 117, 415−421

cellulose sources). Furthermore, crystallite aggregation is enhanced[44] in the experiments because sorption isotherms start from *dried* celluloses.

4.3. Geometric Model of Crystallite Bundles. The primary role of crystallite width and the generally observed aggregation of crystallites into bundles[44−47] lead us to recognize that main inferences should be derived from the cross section of crystallite bundles. Figure 5 presents a cross-section model

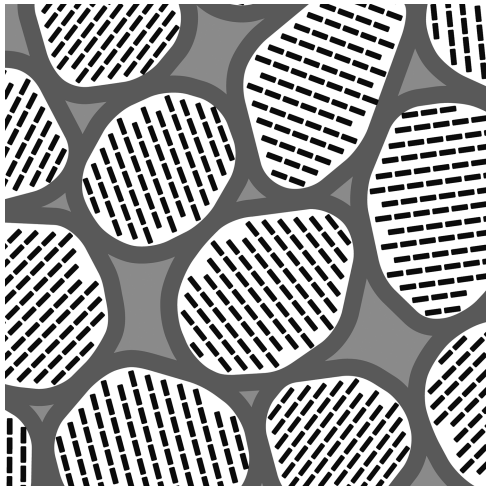

Figure 5. Cross-section model for the interior of a crystallite bundle. Black rectangles represent crystalline cellulose chains. Dark-gray areas are transition layers required to interface mismatched crystallites. Light-gray areas are regions defined by imperfect packing of crystallites. Both gray areas represent disordered hydrated polysaccharides.

for the interior of a crystallite bundle. Cellulose chains belonging to crystallites are represented as black rectangles. Transition layers surrounding crystallites are represented in dark gray. Regions defined by the imperfect packing of crystallites are represented in light gray. Both gray areas represent hydrated polysaccharides.

The layer surrounding crystallites is likely required as a transition to interface paralleled crystallites with mismatched equatorial orientation, i.e., crystallites with different rotations around the long axis, as represented in Figure 5. There is fragmentary experimental evidence[48,49] in favor of random equatorial orientation of cellulose crystallites.

To estimate the volume fraction v_h occupied by hydrated polysaccharides, we consider that the cross-section area of the crystallite is proportional to L^2. The cross-section area of the crystallite plus its surrounding layer (dark gray in Figure 5) of thickness δ is proportional to $(L + 2\delta)^2$. The region defined by the imperfect packing of crystallites (light gray in Figure 5) is considered a constant fraction ε of the area $(L + 2\delta)^2$. This is analogous to the voids among closed-packed cylinders; the cross-section areas of the voids have a constant proportion to those of the cylinders. Taking these considerations, v_h can be written as

$$v_h = \frac{[(L + 2\delta)^2 - L^2] + \varepsilon(L + 2\delta)^2}{(L + 2\delta)^2(1 + \varepsilon)} \quad (2)$$

Expanding eq 2 to first order in δ/L leads to

$$v_h \approx \frac{\varepsilon}{1 + \varepsilon} + \frac{4\delta}{(1 + \varepsilon)}\left(\frac{1}{L}\right) \quad (3)$$

According to eq 3, v_h against $1/L$ is a linear relation with positive intercept and slope. The positive slope is associated with the layer of thickness δ surrounding crystallites (dark gray in Figure 5). This slope is consonant with the positive slope observed in Figures 2 and 4. The positive intercept is due to the fraction ε associated with the light gray areas in Figure 5. If this association is correct, the positive intercepts of Figure 2 indicates that a substantial fraction of ML hydration is associated with polysaccharides in such regions defined by the imperfect packing of aggregated crystallites. Polysaccharide density in these regions may be much lower than in crystallites. However, it is dense enough to block N_2 penetration (in dry samples), as implied by the low (~1 m^2/g) specific areas measured by N_2 sorption.[12,13] The situation may be different in celluloses having much wider crystallites. For instance, a N_2 sorption area of ~100 m^2/g was reported[12] for Cladophora (green algae) cellulose, indicating that in this case N_2 could reach most of the crystallite surfaces.

5. CONCLUSIONS

This article analyzed a wide spectrum of celluloses isolated from plants, having the cellulose I phase, negligible contents of lignin, and variable contents of hemicelluloses. The major finding was a linear relation (R^2 = 0.98) between monolayer hydration (an estimate of water contacting the solid, inferred from vapor sorption) and reciprocal crystallite width (inferred from X-ray diffraction, with modeling of area-detector patterns). As a first point, this observation supported that most water-accessible polysaccharides (cellulose plus hemicelluloses) are laterally associated to cellulose crystallites, with minor fractions (limited to a few percent) left to domains existing along the fibrils.

The main determinant of monolayer water sorption was shown to be structural (crystallite width), not compositional (contents of hemicelluloses), as sometimes assumed. Contents of hemicelluloses were also shown to be secondary for degrees of crystallinity. The secondary role of composition was attributed to the presence of intrinsic disorder at crystallite interfaces. Although disordered interfaces can be found in several cellulose structural models, our results went further to indicate that cellulose is decrystallized to *complement* hemicelluloses, yielding the required amount of disordered interfacial compounds. In this sense, interfacial cellulose can be as "amorphous" and hydrated as are the hemicelluloses.

A geometric model for the cross section of crystallite bundles (also termed macrofibrils or aggregates) was able to explain the observed linear relation between hydration and reciprocal crystallite width. In addition to a layer of disordered, hydrated polysaccharides at crystallite surfaces, we included hydrated polysaccharides in voids left by the imperfect packing of bundled (aggregated) crystallites. This new component explained the positive intercept of monolayer hydration versus reciprocal crystallite width, which corresponded to a substantial fraction of measured monolayer hydration.

■ ASSOCIATED CONTENT

Supporting Information

Comparison between $L_{1\underline{1}0}$, L_{110}, and L_{200}. This material is available free of charge via the Internet at http://pubs.acs.org.

dx.doi.org/10.1021/jp309948h | J. Phys. Chem. B 2013, 117, 415−421

AUTHOR INFORMATION

Corresponding Author

*E-mail: carlos.driemeier@bioetanol.org.br. Phone: +55 19 3518 3180. Fax: +55 19 3518 3164.

Present Address

[†]VTT Brasil − Centro de Pesquisas Técnicas 06455-000, Barueri, São Paulo, Brazil.

Notes

The authors declare no competing financial interest.

ACKNOWLEDGMENTS

Research supported by LNLS − Brazilian Synchrotron Light Laboratory and LNBio − Brazilian Biosciences National Laboratory (project GAR-6293), FAPESP (project 2010/05523-3), and CNPq/PNPD (project 560489/2010-2). The authors thank M. T. B. Pimenta for providing cellulose samples and Danilo B. Mello for artwork.

REFERENCES

(1) Debzi, E. M.; Chanzy, H.; Sugiyama, J.; Tekely, P.; Excoffier, G. *Macromolecules* **1991**, *24*, 6816−6822.

(2) Horii, F.; Yamamoto, H.; Kitamaru, R.; Tanahashi, K.; Higuchi, T. *Macromolecules* **1987**, *20*, 2946−2949.

(3) Nishiyama, Y.; Langan, P.; Chanzy, H. *J. Am. Chem. Soc.* **2002**, *124*, 9074−9082.

(4) Skaar, C. *Wood-water relations*; Springer-Verlag: Berlin, 1988.

(5) Elbaum, R.; Zaltzman, L.; Burgert, I.; Fratzl, P. *Science* **2007**, *316*, 884−886.

(6) Fernandes, A. N.; Thomas, L. H.; Altaner, C. M.; Callow, P.; Forsyth, V. T.; Apperley, D. C.; Kennedy, C. J.; Jarvis, M. C. *Proc. Natl. Acad. Sci. U.S.A.* **2011**, *108*, E1195−1203.

(7) Kennedy, C. J.; Šturcová, A.; Jarvis, M. C.; Wess, T. J. *Cellulose* **2007**, *14*, 401−408.

(8) Müller, M.; Czihak, C.; Schober, H.; Nishiyama, Y.; Vogl, G. *Macromolecules* **2000**, *33*, 1834−1840.

(9) Hailwood, A. J.; Horrobin, S. *Trans. Faraday Soc.* **1946**, *42*, B084−B092.

(10) Hermans, P. H.; Weidinger, A. *J. Appl. Phys.* **1948**, *19*, 491−506.

(11) Hermans, P. H.; Weidinger, A. *J. Polym. Sci.* **1949**, *4*, 317−322.

(12) Mihranyan, A.; Llagostera, A. P.; Karmhag, R.; Strømme, M.; Ek, R. *Int. J. Pharm.* **2004**, *269*, 433−442.

(13) Kocherbitov, V.; Ulvenlund, S.; Kober, M.; Jarring, K.; Arnebrant, T. *J. Phys. Chem. B* **2008**, *112*, 3728−3734.

(14) Strømme, M.; Mihranyan, A.; Ek, R.; Niklasson, G. A. *J. Phys. Chem. B* **2003**, *107*, 14378−14382.

(15) Segal, L.; Creely, J. J.; Martin, A. E., Jr.; Conrad, C. M. *Text. Res. J.* **1959**, *29*, 786−794.

(16) Park, S.; Baker, J. O.; Himmel, M. E.; Parilla, P. A.; Johnson, D. K. *Biotechnol. Biofuels* **2010**, *3*, 10.

(17) Driemeier, C.; Calligaris, G. A. *J. Appl. Crystallogr.* **2011**, *44*, 184−192.

(18) Driemeier, C.; Pimenta, M. T. B.; Rocha, G. J. M.; Oliveira, M. M.; Mello, D. B.; Maziero, P.; Gonçalves, A. R. *Cellulose* **2011**, *18*, 1509−1519.

(19) Hindeleh, A. M.; Johnson, D. J. *Polymer* **1972**, *13*, 423−430.

(20) Olsson, A.-M.; Bjurhager, I.; Gerber, L.; Sundberg, B.; Salmén, L. *Planta* **2011**, *233*, 1277−1286.

(21) Simonović, J.; Stevanic, J.; Djikanović, D.; Salmén, L.; Radotić, K. *Cellulose* **2011**, *18*, 1433−1440.

(22) Wickholm, K.; Larsson, P. T.; Iversen, T. *Carbohydr. Res.* **1998**, *312*, 123−129.

(23) Newman, R. H. *Solid State Nucl. Magn. Resonan.* **1999**, *15*, 21−9.

(24) Ioelovitch, M. *Acta Polym.* **1992**, *43*, 110−113.

(25) Leppänen, K.; Andersson, S.; Torkkeli, M.; Knaapila, M.; Kotelnikova, N.; Serimaa, R. *Cellulose* **2009**, *16*, 999−1015.

(26) Cosgrove, D. J. *Nat. Rev. Mol. Cell Biol.* **2005**, *6*, 850−861.

(27) Müller, M.; Burghammer, M.; Sugiyama, J. *Holzforschung* **2006**, *60*, 474−479.

(28) Pimenta, M. T. B. *Utilização de fluidos nos estados sub/supercrítico na polpação de Eucalyptus grandis e Pinus taeda*; Universidade de São Paulo: São Carlos, Brazil, 2005.

(29) Sluiter, A.; Hames, B.; Ruiz, R.; Scarlata, C.; Sluiter, J.; Templeton, D.; Crocker, D. *Determination of structural carbohydrates and lignin in biomass*; Technical Report NREL/TP-510-42618, 2008.

(30) Rietveld, H. M. *J. Appl. Crystallogr.* **1969**, *2*, 65−71.

(31) Ferrari, M.; Lutterotti, L. *J. Appl. Phys.* **1994**, *76*, 7246−7255.

(32) Delhez, R.; de Keijser, T. H.; Langford, J. I.; Louër, D.; Mittemeijer, E. J.; Sonneveld, E. J. In *The Rietveld Method*; Young, R. A., Ed.; Oxford University Press: New York, 1993; pp 132−166.

(33) Driemeier, C.; Mendes, F. M.; Oliveira, M. M. *Cellulose* **2012**, *19*, 1051−1063.

(34) Brunauer, S.; Emmett, P. H.; Teller, E. *J. Am. Chem. Soc.* **1938**, *60*, 309−319.

(35) Bragatto, J.; Segato, F.; Cota, J.; Mello, D. B.; Oliveira, M. M.; Buckeridge, M. S.; Squina, F. M.; Driemeier, C. *J. Phys. Chem. B* **2012**, *116*, 6128−6136.

(36) Kocherbitov, V.; Arnebrant, T. *Langmuir* **2009**, *26*, 3918−3922.

(37) Roe, R.-J. *Methods of X-ray and Neutron Scattering in Polymer Science*; Oxford University: New York, 2000.

(38) Ioelovich, M.; Leykin, A.; Figovsky, O. *BioResources* **2010**, *5*, 1393−1407.

(39) Hosemann, R.; Hindeleh, A. M. *J. Macromol. Sci., Part B: Phys.* **1995**, *B34*, 327−356.

(40) Nishiyama, Y.; Kim, U.-J.; Kim, D.-Y.; Katsumata, K. S.; May, R. P.; Langan, P. *Biomacromolecules* **2003**, *4*, 1013−1017.

(41) Samir, M. A. S. A.; Alloin, F.; Dufresne, A. *Biomacromolecules* **2005**, *6*, 612−626.

(42) Elazzouzi-Hafraoui, S.; Nishiyama, Y.; Putaux, J.-L.; Heux, L.; Dubreuil, F.; Rochas, C. *Biomacromolecules* **2008**, *9*, 57−65.

(43) Teixeira, E. M.; Bondancia, T. J.; Teodoro, K. B. R.; Corrêa, A. C.; Marconcini, J. M.; Mattoso, L. H. C. *Ind. Crops Prod.* **2011**, *33*, 63−66.

(44) Hult, E.-L.; Larsson, P. T.; Iversen, T. *Polymer* **2001**, *42*, 3309−3314.

(45) Fahlén, J.; Salmén, L. *Biomacromolecules* **2005**, *6*, 433−438.

(46) Zhao, H.; Kwak, J. H.; Zhang, Z. C.; Brown, H. M.; Arey, B. W.; Holladay, J. E. *Carbohydr. Polym.* **2007**, *68*, 235−241.

(47) Donaldson, L. *Wood Sci. Technol.* **2007**, *41*, 443−460.

(48) Revol, J.-F.; Gancet, C.; Goring, D. A. I. *Wood Sci.* **1982**, *14*, 120−126.

(49) Näslund, P.; Vuong, R.; Chanzy, H.; Jésior, J. C. *Text. Res. J.* **1988**, *58*, 414−417.